POLITECNICO
MILANO 1863

SCUOLA DI INGEGNERIA INDUSTRIALE
E DELL'INFORMAZIONE

Executive Summary of the Thesis

Lumped-parameter models for the simulation of cardiovascular congenital diseases

Laurea Magistrale in Aeronautical Engineering - Ingegneria Aeronautica

Author: Giulio Valenti

Advisor: Prof. Luca Dedè

Co-advisors: Andrea Tonini; Paolo Ferrero, MD; Prof. Alfio Quarteroni

Academic year: 2022-2023

1. Introduction

Congenital heart defects represent a category that includes numerous diseases that vary widely from each other. The objective through this study is to construct a mathematical model that can simulate the cardiac circulation of patients affected by these diseases.
The aim of these models is to improve the physiological understandings of the diseases and possibly to support the medical staff on taking the best decision for the patient.
The studied congenital defects are the patent foramen ovale (PFO), the partial anomalous pulmonary venous return (PAPVR), the atrial septal defect (ASD) and the ventricular septal defect (VSD).
We propose the implementation of these diseases in a 0D lumped-parameters model previously calibrated to produce clinical outputs in a healthy range. The used lumped-parameters model, inspired by [1, 2, 4], exploits the analogy between the cardiac circulation vessels system and an electrical circuit, Figure 1.
PFO was implemented by using a Bernoulli valve model, [3]. PAPVR was simulated by firstly splitting the reference model pulmonary venous compartment into the four pulmonary veins and subsequently connecting the pulmonary veins in two different anomalous spots: the right atrium and the superior vena cava.
ASD and VSD were implemented as two electical resistances connecting the respective heart chambers. For these two septa defects we also performed a model calibration for three different patients, whom clinical data have been provided by Dott. Paolo Ferrero (IRCCS Policlinico San Donato Hospital, Italy).

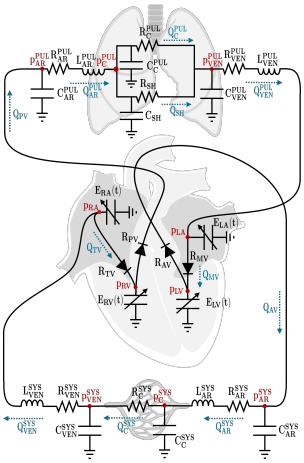

Figure 1: Lumped-parameter cardiocirculatory model.

The model with the PFO implementation is able

to estimate an increasing impact on the circulation for increasing foramen radius.
PAPVR simulation predicts an increasing impact by progressively increasing the anomalous veins number. In addition, it correctly estimates a lower impact in the case of anomalous attachment to the superior vena cava with respect to the case with anomalous attachment directly into the right atrium.
Finally for the septa defects, the model calibration highlighted a critical effect on the patients lumped-parameters due to the abnormal circulation pattern endured over time.

2. Mathematical methods

The electrical analogy simulates the blood vessels systems, current represents blood flow rate and the electrical potential blood pressure.
For each electrical segment the electric resistance simulates the viscous resistance of blood flow and the resistance of vessel wall, the capacitance reflects the vessel compliance and the inductance measure the resistance to changes in blood flow.
We used an arterial, a venous and a capillary electrical RLC compartment to model both systemic and pulmonary circulations [2, 4]. The pulmonary capillaries are further divided into oxygenated and non-oxygenated ones. Each vessel pressure and flow are regulated by the following equations.

$$\begin{aligned} L\frac{dQ_o}{dt} + RQ_o &= P_i - P_o, \\ C\frac{d(P_i - p_{ex})}{dt} &= Q_i - Q_o \end{aligned} \tag{1}$$

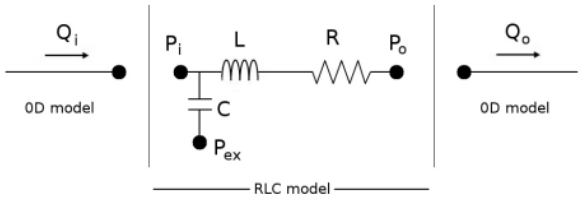

Figure 2: Electrical segment, i:input, o:output.

The cardiac valves are modeled as non ideal diodes, their resistance depend on their Pre-valve and Post-valve pressures:

$$R_i(p_1, p_2) = \begin{cases} R_{min} & \text{if } p_1 > p_2 \\ R_{max} & \text{if } p_1 \leq p_2 \end{cases} \tag{2}$$

where p_1 and p_2 represent the upstream and downstream pressures with respect to the flow direction, whereas R_{min} and R_{max} are the minimum and maximum resistance of the valves.
The cardiac chambers are modeled with 0-dimensional elastance relationships [1]:

$$p_i(t) = p_{ex}(t) + E_{ch}(t)(V_{ch} - V_{0,ch}) \tag{3}$$

where $p_i(t)$ is the considered chamber pressure, $p_{ex}(t)$ represents the external (to the heart) pressure exerted by the surrounding organs and respiration, $V_{ch}(t)$ is the cardiac volume of the chamber and $V_{0,ch}$ refers to the blood unstressed volume of such chamber.
The general elastance formula is:

$$E_{ch}(t) = E_A e(t) + E_B \tag{4}$$

The two parameters E_A and E_B, different for every cardiac chambers, are respectively called active and passive elastance. $e(t)$ is a normalized, time-varying and periodic function that regulates the elastance oscillating behaviour during the heartbeat. This term differ between atria and ventricle by just a time translation.
By setting the continuity equations of flow rates at the circuit nodes and of pressure in the vessels it can be obtained the resulting system of ODEs regulating lumped-parameters model, Eq. 6.
In the PFO and PAPVR simulations we used the ode15s from in MATLAB. This solver implements a variable step, variable order method based on the implicit family of backward differentiation formula methods. For the calibration process we used the L-BFGS-B algorithm to minimize a loss function which measures the discrepancy between clinical data and the calibrated model outputs.
During the calibration process the resolution of the model ODEs system was computed by approximating its solution using Dormand-Prince, an embeeded Runge-Kutta method that calculate fourth and fifth order accurate solutions.
Considering the large number of parameters, we identified the ones which affected more the model outputs reproducing the available clinical data by using the total Sobol' indices:

$$S_{T_i} = 1 - \frac{Var_{\mathbf{X}\sim i}(E_{Xi}(Y|\mathbf{X}_{\sim i}))}{Var(Y)} \tag{5}$$

These indices measure for each model output how it is affected by each model input.

$$
\begin{cases}
C_{VEN}^{SYS}\dfrac{dp_{VEN}^{SYS}}{dt} = Q_{AR}^{SYS} - Q_{VEN}^{SYS} \\
C_{VEN}^{PUL}\dfrac{dp_{VEN}^{PUL}}{dt} = Q_{AR}^{PUL} - Q_{VEN}^{PUL} \\
\dfrac{L_{VEN}^{SYS}}{R_{VEN}^{SYS}}\dfrac{dQ_{VEN}^{SYS}}{dt} = -Q_{VEN}^{SYS} - \dfrac{p_{RA} - p_{VEN}^{SYS}}{R_{VEN}^{SYS}} \\
\dfrac{L_{VEN}^{PUL}}{R_{VEN}^{PUL}}\dfrac{dQ_{VEN}^{PUL}}{dt} = -Q_{VEN}^{PUL} - \dfrac{p_{LA} - p_{VEN}^{PUL}}{R_{VEN}^{PUL}} \\
\dfrac{dV_{RA}}{dt} = Q_{VEN}^{SYS} - Q_{TV}(p_{RA}, p_{RV}) \\
\dfrac{dV_{LA}}{dt} = Q_{VEN}^{PUL} - Q_{MV}(p_{LA}, p_{LV}) \\
\dfrac{dV_{RV}}{dt} = Q_{TV}(p_{RA}, p_{RV}) - Q_{PV}(p_{RV}, p_{AR}^{PUL}) \\
\dfrac{dV_{LV}}{dt} = Q_{MV}(p_{LA}, p_{LV}) - Q_{AV}(p_{LV}, p_{AR}^{SYS}) \\
C_{AR}^{PUL}\dfrac{dp_{AR}^{PUL}}{dt} = Q_{PV}(p_{RV}, p_{AR}^{PUL}) - Q_{AR}^{PUL} \\
C_{AR}^{SYS}\dfrac{dp_{AR}^{SYS}}{dt} = Q_{AV}(p_{LV}, p_{AR}^{SYS}) - Q_{AR}^{SYS} \\
\dfrac{L_{AR}^{PUL}}{R_{AR}^{PUL}}\dfrac{dQ_{AR}^{PUL}}{dt} = -Q_{AR}^{PUL} - \dfrac{p_{VEN}^{PUL} - p_{AR}^{PUL}}{R_{AR}^{PUL}} \\
\dfrac{L_{AR}^{SYS}}{R_{AR}^{SYS}}\dfrac{dQ_{AR}^{SYS}}{dt} = -Q_{AR}^{SYS} - \dfrac{p_{VEN}^{SYS} - p_{AR}^{SYS}}{R_{AR}^{SYS}} \\
C_{C}^{SYS}\dfrac{dp_{C}^{SYS}}{dt} = Q_{AR}^{SYS} - Q_{C}^{SYS}(p_{C}^{SYS}, p_{VEN}^{SYS}) \\
\dfrac{dp_{C}^{PUL}}{dt} = \dfrac{Q_{AR}^{PUL} - Q_{SH}(p_{C}^{PUL}, p_{VEN}^{PUL}) - Q_{C}^{PUL}(p_{C}^{PUL}, p_{VEN}^{PUL})}{(C_{C}^{PUL} + C_{SH})}
\end{cases}
\tag{6}
$$

3. Defects anatomy and implementation

3.1. PFO

The foramen is a flap like opening, necessary for the fetal circulation that should close by itself the first year of life. The conditions in which it persits, is called PFO. It is composed of a first free strip of interatrial septal tissue that moves into the left atrium and a second fixed strip of tissue belonging to the interatrial septa. When the left atrium pressure is higher than the right one the free strip is pressed against the fixed strip, closing the orifice. In contrast, with higher pressure in the right atrium the orifice is opened and blood moves from the right atrium to the left one. This abnormal blood movement is called shunt.

Pulmonary arterial constriction (with a constricted-to-healthy radius ratio of 0.8) is simulated to achieve a right to left atrium positive pressure gradient.

The PFO was modeled by using a Bernoulli valve model:

$$\Delta p = R_{PFO}^{B} q|q| + L_{PFO}\frac{dq}{dt} \tag{7}$$

Δp and q are the pressure gradient and blood flow across the valve. R_{PFO}^{B} and L_{PFO} are respectively called Bernoulli resistance and inertance and regulate the dynamic and viscous pressure losses. Considering a positive shunt flow for blood moving through the PFO from the right atrium to left one the model and the atrial volume equations can be modified as follow:

$$
\begin{cases}
\dfrac{dV_{RA}}{dt} = Q_{VEN}^{SYS} - Q_{TV} - Q_{PFO}(p_{RA}, p_{LA}) \\
\dfrac{dV_{LA}}{dt} = Q_{VEN}^{PUL} - Q_{MV} + Q_{PFO}(p_{RA}, p_{LA})
\end{cases}
\tag{8}
$$

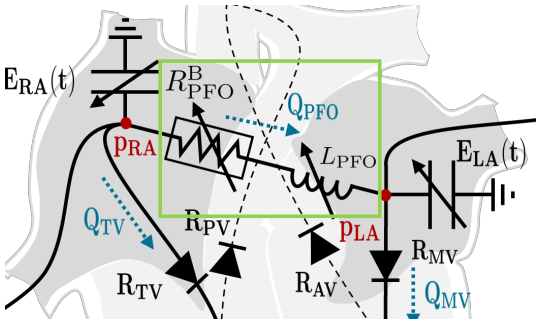

Figure 3: PFO implementation

3.2. PAPVR

PAPVR is an anomalous connection in which the pulmonary veins drain in the right atrium or in its tributaries instead that normally moving blood to the left atrium. The oxygenated blood flowing through these anomalous pulmonary veins shunt in the right atrium, and subsequently is pushed again in the pulmonary circulation. This circulation anomaly decreases the oxygenated blood replenishing the body through the systemic circulation.

We firstly divided the pulmonary venous compartment of the healthy reference into the four main pulmonary veins using the equivalent formulas for parallel circuits. Then, we progressively connected more of these veins into an anomalous spot. We repeated this simulation for two anomalous spots: the right atrium and the superior vena cava (SVC).

The atrial volume equations for the atrium case become:

$$\begin{cases} \dfrac{dV_{LA}}{dt} = \displaystyle\sum_{i=1}^{N_i} Q^{PUL}_{VEIN,i} - Q_{MV}(p_{LA}, p_{LV}) \\ \dfrac{dV_{RA}}{dt} = Q^{SYS}_{VEN} + \displaystyle\sum_{j=1}^{N_j} Q^{PUL}_{VEIN,j} - Q_{TV}(p_{RA}, p_{RV}) \end{cases} \tag{9}$$

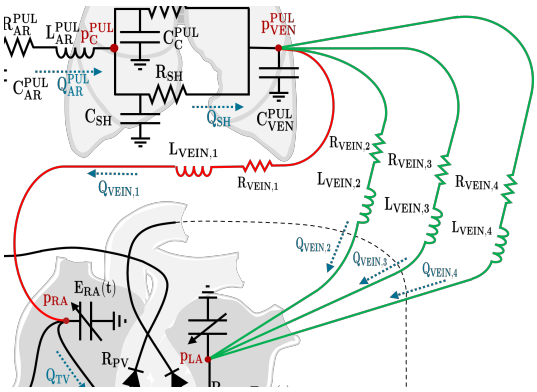

Figure 4: PAPVR implementation: atrium case

Where N_i is the number of normal veins colored in green, whereas N_j is the number of anomalous veins colored in red.
In the second case however, before moving to the right atrium the shunting blood first enters the SVC . The left ventricular volume equation is unchanged.

$$\begin{cases} C_{SVC}\dfrac{dp_{SVC}}{dt} = Q^{SYS}_{VEN} + \displaystyle\sum_{j=1}^{N_j} Q^{PUL}_{VEIN,j} - Q_{SVC} \\ \dfrac{L_{SVC}}{R_{SVC}}\dfrac{dQ_{SVC}}{dt} = -Q_{SVC} - \dfrac{p_{RA} - p_{SVC}}{R_{SVC}} \\ \dfrac{dV_{RA}}{dt} = Q_{SVC} - Q_{TV}(p_{RA}, p_{RV}) \end{cases} \tag{10}$$

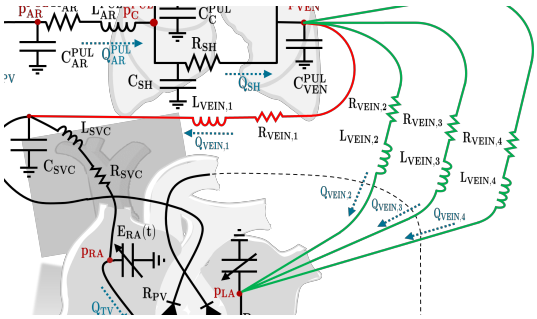

Figure 5: PAPVR implementation: SVC case

3.3. ASD/VSD

Each septal defect is characterized by a hole that puts in communication the adjacent respective cardiac chambers (atria or ventricles).
Depending on the pressure between the two chambers the blood is pushed through the hole and overload the receiving atrium/ventricle. As a consequence one of the two circulation system receives less blood, whereas the other is overloaded by more blood.
They have been modeled as two resistances as in the Figure 6.

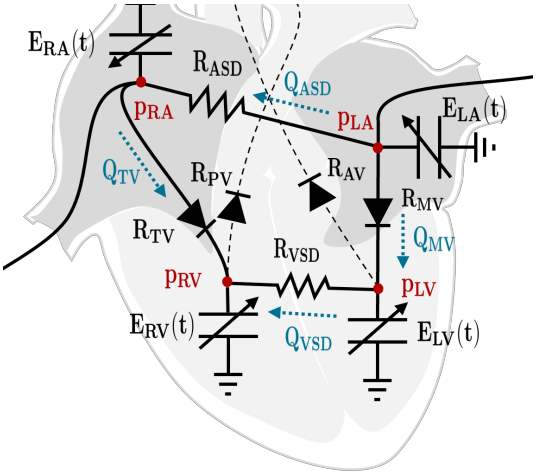

Figure 6: ASD and VSD implementation example

We define the shunting flow through the septal defects as positive for blood moving from the left compartments to the right ones. In ASD presence the atrial volume equations become:

$$\begin{cases} \dfrac{dV_{RA}}{dt} = Q^{SYS}_{VEN} - Q_{TV}(p_{RA}, p_{RV}) - Q_{ASD}(p_{LA}, p_{RA}) \\ \dfrac{dV_{LA}}{dt} = Q^{PUL}_{VEN} - Q_{MV}(p_{LA}, p_{LV}) + Q_{ASD}(p_{LA}, p_{RA}) \end{cases}$$

Whereas in VSD presence the ventricular volume equations become:

$$\begin{cases} \dfrac{dV_{RV}}{dt} = Q_{TV} - Q_{PV}(p_{RV}, p^{PUL}_{AR}) + Q_{VSD}(p_{LV}, p_{RV}) \\ \dfrac{dV_{LV}}{dt} = Q_{MV} - Q_{PV}(p_{LV}, p^{SYS}_{AR}) - Q_{VSD}(p_{LV}, p_{RV}) \end{cases}$$

If the studied patient presents both defects, all the cardiac chambers' volume equations have to be modified as in the singular septa defect cases just presented.

4. Results

By enlarging the foramen radius, the model predict an increase on the blood shunt flow, more blood is subtracted by the right heart and moved by the left heart in the systemic circulation. From the mean pulmonary and systemic flows it can be computed a shunt ratio that works as severity indicator. The farther this ratio is from one, the higher the impact caused by the defect on the cardiac circulation, see Table 1.

Table 1: Foramen model results

Foramen radius	$\frac{Q_P}{Q_S}$
$r_{small} = 5.0\ mm$	0.9598
$r_{medium} = 9.0\ mm$	0.9442
$r_{large} = 13.0\ mm$	0.9438

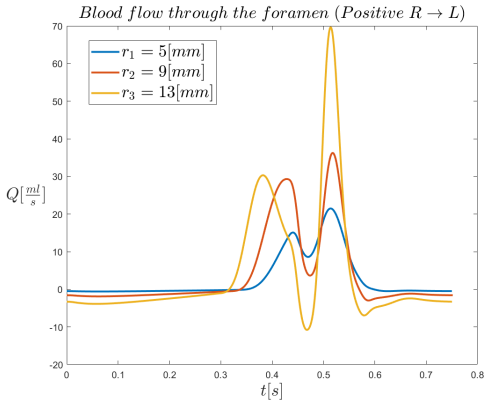

Figure 7: Shunting flows through PFO

Considering the PAPVR results of the atrium case it can be seen that the blood volumes moving through the anomalous veins in a heartbeat V^{HB}_{VEIN} slightly decrease by moving from the single do the double anomalous veins scenario.
In contrast, by moving to the triple anomalous veins scenario, both the flow curve and the volume of blood moving through the anomalous veins greatly increase.

Table 2: PAPVR: atrium case shunt ratios

Case	$\frac{Q_P}{Q_S}$	$V^{HB}_{VEIN}\ [ml]$
1 *anomalous vein*	1.3362	20.83
2 *anomalous veins*	1.7276	20.7
3 *anomalous veins*	2.5696	25.1

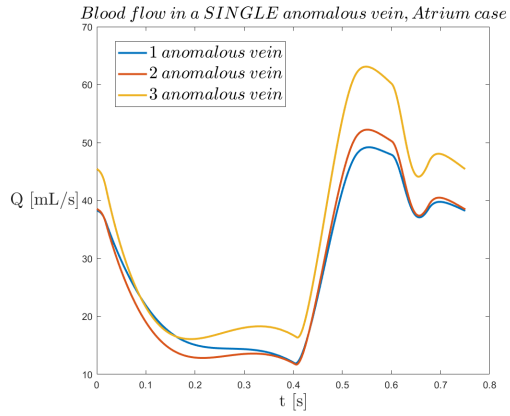

Figure 8: Shunting blood flows, atrium case

The right atrium and consequently the right ventricle receives more blood from the anomalous veins. The right ventricle gets progressively overloaded and its pressure and end diastolic volume greatly increase.

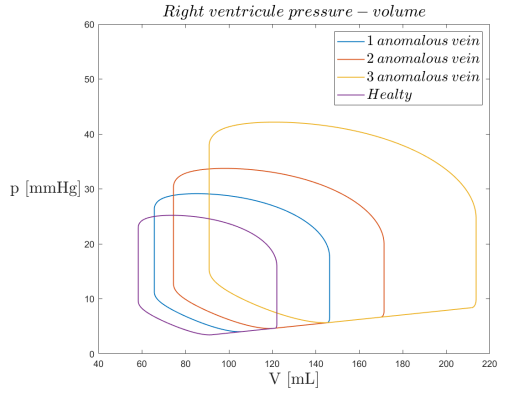

Figure 9: Right ventricular P-V loop

In the anomalous connection to the SVC case, the blood shunting volume slightly increase passing from single to double anomalous veins. In line with the atrium case, Table 2, the shunting blood and volume greatly increase passing to the triple anomalous veins scenario.

Table 3: PAPVR: SVC case shunt ratios

Case	$\frac{Q_P}{Q_S}$	$V^{HB}_{VEIN}\ [ml]$
1 *anomalous vein*	1.2475	15.16
2 *anomalous veins*	1.5467	15.34
3 *anomalous veins*	2.2241	19.31

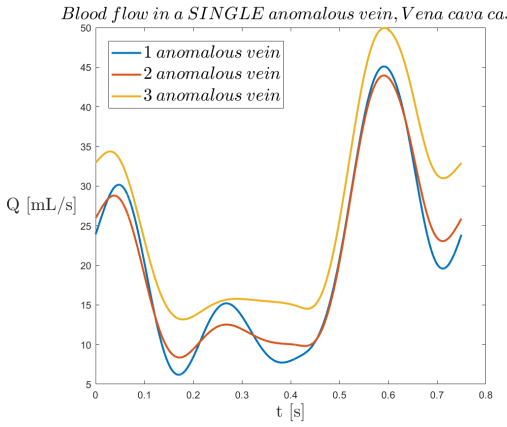

Figure 10: Shunting blood flows, SVC case

As expected the shunt ratios and volumes are globally inferior compared to the atrium case. The connection spot in the superior vena cava is at higher pressure compared to the right atrium. This implies that the pressure gradient between anomalous veins origin and downstream connection spot is lower. As a consequence the blood flowing through them must decrease.

Looking at the model calibrations, the resulting pulmonary resistances are considerably larger than the healthy reference ones in the second and in the third patient, in other words those with the VSD, Table 4.
In healthy conditions, the left ventricular pressure is considerably higher than the right one. This implies that in VSD presence an important quantity of blood moves from the left to the right ventricle. This already oxygenated blood is again pushed in the pulmonary circulation, overloading it and putting under structural stress its vessels.
The body stimulated by this pulmonary hypertension tries to adapt through a cellular proliferation, which narrows the pulmonary vessels and consequently increases their resistance.
The increased resistance reduces the pulmonary flow, helping the body in the rebalancing of its cardiac circulation.
Another important parameter change is the arterial pulmonary capacitance. Probably due to the same reason, the mechanical stress upon the pulmonary artery strains over time its tissues. The vessel lose elasticity and consequently its ability to dilate to store pressure as potential elastic energy.

Table 4: Model calibrations resulting parameters comparisons

Parameter	R_{AR}^{PUL}	R_{VEN}^{PUL}	C_{AR}^{PUL}
Healty	0.0714	0.0375	6.004
ASD	0.079	0.003	3.095
VSD	0.382	0.216	0.8124
VSD/VD	0.152	0.143	0.81
ASD/VSD	0.351	0.05	0.586
Units	$\frac{mmHgs}{ml}$	$\frac{mmHgs}{ml}$	$\frac{ml}{mmHg}$

5. Conclusions

We modified a 0D lumped-parameter model by introducing the PFO. The obtained model correctly estimates an increasing severity behaviour for larger defects. In particular it correctly estimates shunt ratios close to the healthy value of 1, suggesting a global low impact on the cardiac circulation. Indeed the defect is present in a quarter of the world population and mostly of them are unaffected in their daily activities.
Subsequently we reshaped the starting model to simulate the PAPVR disease. The resulting model estimates shunt ratios larger than the healthy value of one, therefore predicting a pulmonary circulation overload. In addition, these shunt rarios are farther away from the healthy value than in the PFO simulations, suggesting a more significant global impact on the cardiac circulation.
The PFO and PAPVR customized models have not been calibrated on patients affected by these diseases, and therefore it is not possible to correctly predict if and how the body has adapted over time to these defects.
Finally, we introduced the septa defects as resistances in the starting model. We performed a parameters calibration on the resulting models, using clinical data from three different patients. The calibration process highlighted an adaptation process that permanently changed the circulation structure.
However, this patient-specific calibration took a lot of time (approximately 20 days). In its current state, this procedure is too slow compared to the timing required in the medical field.
The calibration process can be accelerated by integrating in the procedure software or machine

learning-based methods that exploit considerations based on the patient clinical data to improve the initial guess on the patient parameters.

References

[1] Pablo J Blanco and Raúl A Feijóo. A 3d-1d-0d computational model for the entire cardiovascular system. *Mecánica Computacional*, 29(59):5887–5911, 2010.

[2] Marc Hirschvogel, Marina Bassilious, Lasse Jagschies, Stephen M Wildhirt, and Michael W Gee. A monolithic 3d-0d coupled closed-loop model of the heart and the vascular system: experiment-based parameter estimation for patient-specific cardiac mechanics. *International journal for numerical methods in biomedical engineering*, 33(8):e2842, 2017.

[3] JP Mynard, MR Davidson, DJ Penny, and JJ2946553 Smolich. A simple, versatile valve model for use in lumped parameter and one-dimensional cardiovascular models. *International Journal for Numerical Methods in Biomedical Engineering*, 28(6-7):626–641, 2012.

[4] Francesco Regazzoni, Matteo Salvador, Pasquale Claudio Africa, Marco Fedele, Luca Dedè, and Alfio Quarteroni. A cardiac electromechanical model coupled with a lumped-parameter model for closed-loop blood circulation. *Journal of Computational Physics*, 457:111083, 2022.